Cell Host & Microbe
Article

PPARγ-Mediated Increase in Glucose Availability Sustains Chronic *Brucella abortus* Infection in Alternatively Activated Macrophages

Mariana N. Xavier,[1,4] Maria G. Winter,[1,6] Alanna M. Spees,[1,6] Andreas B. den Hartigh,[1] Kim Nguyen,[1] Christelle M. Roux,[1] Teane M.A. Silva,[4] Vidya L. Atluri,[1] Tobias Kerrinnes,[1] A. Marijke Keestra,[1] Denise M. Monack,[5] Paul A. Luciw,[2] Richard A. Eigenheer,[3] Andreas J. Bäumler,[1] Renato L. Santos,[4] and Renée M. Tsolis[1,*]
[1]Department of Medical Microbiology and Immunology, School of Medicine
[2]Center for Comparative Medicine
[3]Proteomics Core Facility, UC Davis Genome Center
University of California, Davis, Davis, CA 95616, USA
[4]Departamento de Clinica e Cirurgia Veterinarias, Escola de Veterinaria, Universidade Federal de Minas Gerais, 31270-901 Belo Horizonte, MG, Brazil
[5]Department of Microbiology and Immunology, School of Medicine, Stanford University, Palo Alto, CA 94305, USA
[6]These authors contributed equally to this work
*Correspondence: rmtsolis@ucdavis.edu
http://dx.doi.org/10.1016/j.chom.2013.07.009

SUMMARY

Eradication of persistent intracellular bacterial pathogens with antibiotic therapy is often slow or incomplete. However, strategies to augment antibiotics are hampered by our poor understanding of the nutritional environment that sustains chronic infection. Here we show that the intracellular pathogen *Brucella abortus* survives and replicates preferentially in alternatively activated macrophages (AAMs), which are more abundant during chronic infection. A metabolic shift induced by peroxisome proliferator-activated receptor γ (PPARγ), which increases intracellular glucose availability, is identified as a causal mechanism promoting enhanced bacterial survival in AAMs. Glucose uptake was crucial for increased replication of *B. abortus* in AAMs, and for chronic infection, as inactivation of the bacterial glucose transporter *gluP* reduced both intracellular survival in AAMs and persistence in mice. Thus, a shift in intracellular nutrient availability induced by PPARγ promotes chronic persistence of *B. abortus* within AAMs, and targeting this pathway may aid in eradicating chronic infection.

INTRODUCTION

Brucella abortus is a zoonotic bacterial pathogen that establishes long-term infections in its host. In vivo, bacteria are found in association with phagocytic cells, most prominently macrophages, in which a subset of *B. abortus* is able to evade killing in phagolysosomes. Instead, bacteria replicate with an endoplasmic reticulum-associated compartment and interact subsequently with a modified autophagy pathway to promote cell-to-cell spread (Gorvel and Moreno, 2002; Starr et al., 2008). While studies on the interaction between *B. abortus* and macrophages have yielded critical insights into how *B. abortus* survives intracellularly, a subset of factors required for chronic persistence in vivo do not appear to mediate intracellular replication in cultured macrophages (Fretin et al., 2005; Hong et al., 2000), raising the possibility that the niche for chronic bacterial persistence has different characteristics from macrophages cultured in vitro.

Recently, it has been recognized that like other immune cells, macrophages can adopt different functional states that are influenced by the immune microenvironment (reviewed by Gordon and Martinez, 2010; Van Dyken and Locksley, 2013). Activation by interferon gamma (IFNγ) leads to the classically activated macrophage (CAM) phenotype, characterized by production of nitric oxide (NO) and inflammatory cytokines such as tumor necrosis factor alpha (TNF-α) and interleukin-6 (IL-6). During inflammation, these cells can arise from Ly6C^{high} inflammatory monocytes that leave the bone marrow in a CCR2-dependent manner (Shi and Pamer, 2011). In contrast, the Th2 cytokines interleukin-4 (IL-4) and IL-13 activate signal transducer and activator of transcription 6 (STAT6) to promote development of alternatively activated macrophages (AAMs), which play important roles in allergic inflammation, helminth infection, and tissue repair (Lawrence and Natoli, 2011; Reyes and Terrazas, 2007; Shirey et al., 2008). These macrophages express low levels of the inflammatory monocyte marker LY6C.

In addition to roles in inflammation and immunity, CAMs and AAMs play important roles in host physiology and metabolism (reviewed by Chawla, 2010). Development of the AAM phenotype is dependent on peroxisome proliferator-activated receptors (PPARs; Odegaard et al., 2007), which act downstream of STAT6 signaling to regulate macrophage metabolism. Interestingly, our previous results (Hong et al., 2000) implicated bacterial metabolism as key to chronic *B. abortus* infection. Therefore, we sought to investigate the relative importance of AAMs and CAMs as niches for persistent infection, and to determine whether the different metabolic programming of these two macrophage populations contributes to chronic infection by *B. abortus*.

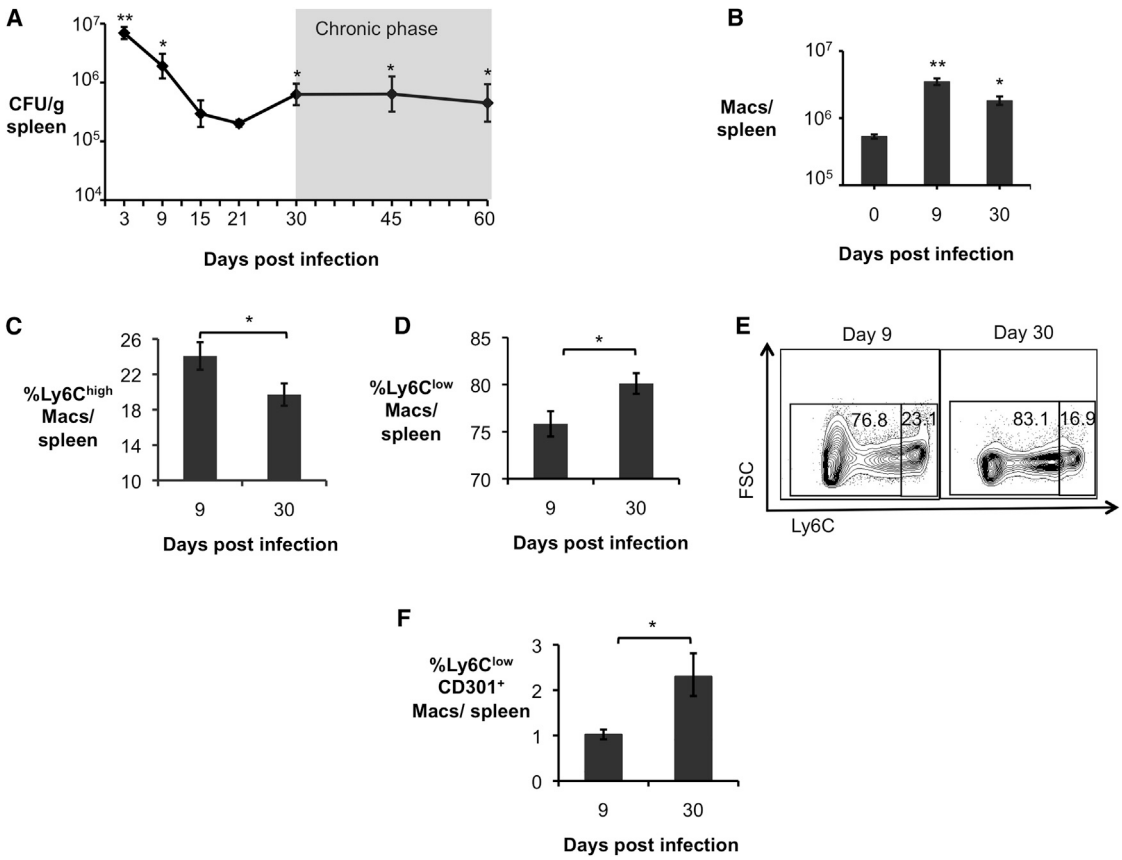

Figure 1. Alternatively Activated Macrophages Are More Abundant during Chronic Brucellosis

(A) *B. abortus* 2308 CFU counts in spleens from C57BL/6J mice (n = 5) at 3, 9, 15, 21, 30, 45, and 60 days postinfection (dpi).

(B) Numbers of macrophages ($CD3^-B220^-NK1.1^-Ly6G^-CD11b^+F4/80^+$) determined by flow cytometry in spleens of *B. abortus*-infected mice (n = 4) at 0, 9, and 30 dpi.

(C) Frequency of $CD3^-B220^-NK1.1^-Ly6G^-CD11b^+F4/80^+Ly6C^{high}$ macrophages (CAM) measured by flow cytometry in spleens of *B. abortus*-infected mice (n = 4) at 9 and 30 dpi.

(D) Frequency of $CD3^-B220^-NK1.1^-Ly6G^-CD11b^+F4/80^+Ly6C^{low}$ macrophages determined by flow cytometry in spleens of *B. abortus*-infected mice (n = 4) at 9 and 30 dpi.

(E) Representative data plot of $Ly6C^{low}$ and $Ly6C^{high}$ populations in spleens of *B. abortus*-infected mice at 9 and 30 dpi. FSC, forward scatter.

(F) Frequency of $CD3^-B220^-NK1.1^-Ly6G^-CD11b^+F4/80^+Ly6C^{low}CD301^+$ macrophages (AAM) measured by flow cytometry in spleens of *B. abortus*-infected mice (n = 4) at 9 and 30 dpi. Values represent mean ± SEM. *$p < 0.05$ and **$p < 0.01$ using one way ANOVA for (A) and (B) or unpaired t test analysis for (C)–(E). See also Figure S1.

RESULTS

Alternatively Activated Macrophages Are More Abundant during Chronic *B. abortus* Infection Compared to Acute Infection

To gain insight into the role of different macrophage populations during different phases of *B. abortus* infection, we performed an infection time course experiment. These results showed that early (1–3 day) bacterial numbers increased, then subsequently declined over the next 21 days, and we designated this as the acute phase of infection. Between 30 and 60 days postinfection, bacterial numbers remained constant, and this was designated the chronic infection phase (Figure 1A). During the acute phase of infection, a short-lived Th1 response (Fernandes et al., 1996) and an influx of inflammatory macrophages (Copin et al., 2012) act to control bacterial colonization. However, while *B. abortus* is found within CAMs early during infection, the intracellular niche for *B. abortus* during the persistence phase is unknown. To shed light on this question, we compared expression of markers of AAMs (Figure 1 and see Figure S1 online) and CAMs (Figure S1) in the spleen, a site of systemic *B. abortus* persistence, during acute and chronic infection. While markers of classical macrophage activation, such as *Nos2* (encoding inducible nitric oxide synthase), *Il6* (encoding interleukin-6), and *Tnfa* (encoding tumor necrosis factor alpha), were elevated in splenic macrophages ($CD11b^+$ cells) during the acute phase of infection, expression of these markers declined during persistent infection (Figure S1A). Further, while the total number of macrophages in the spleen was increased in both acute and chronic infection compared to uninfected mice (Figure 1B), a significantly greater proportion of these macrophages had an inflammatory phenotype during acute infection, as evidenced by their $Ly6C^{high}$ phenotype (Figures 1C and 1E), and low expression of AAM markers *Ym1* and *Fizz1* (Figures S1B and S1C).

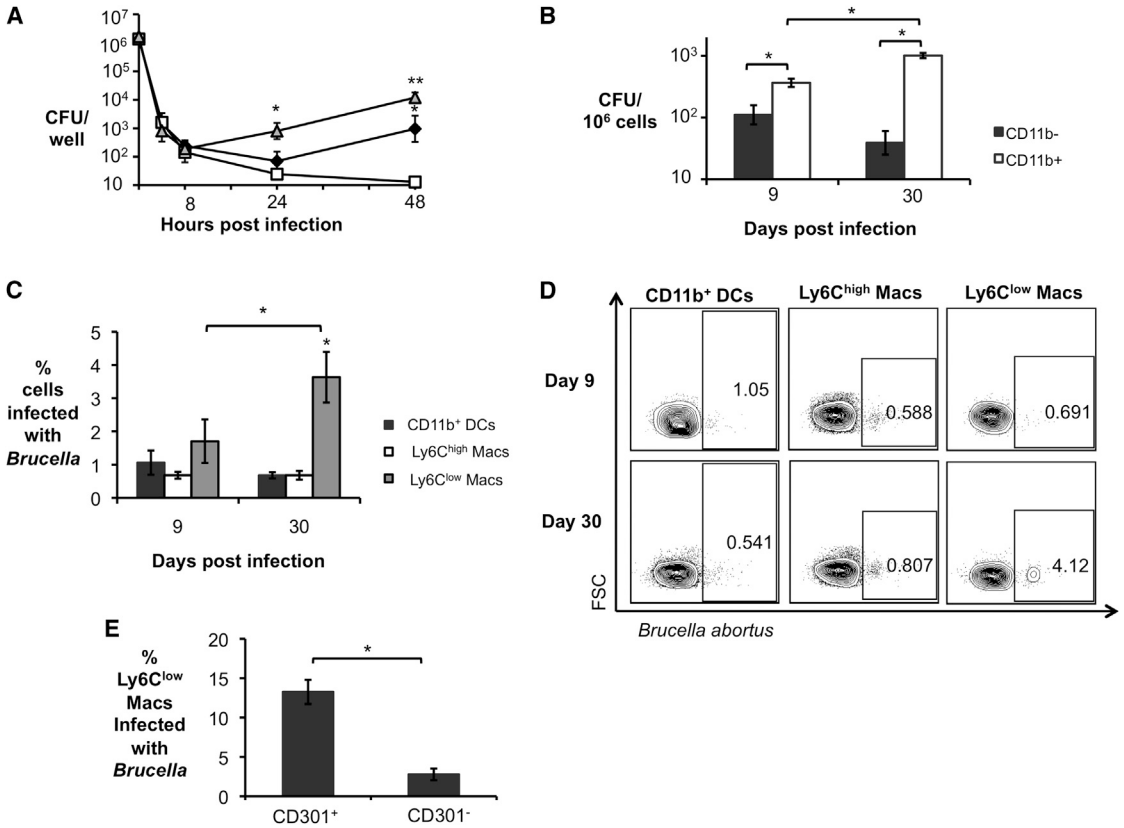

Figure 2. Increased *B. abortus* Survival in AAMs during Chronic Infection

(A) *B. abortus* survival over time in C57BL/6J BMDMs that were not treated (black diamond), or were stimulated with 10 ng/mL of rIFNγ (CAM, open square) and stimulated with 10 ng/mL of rIL-4 (AAM, gray triangle). Data shown are compiled from four independent experiments.

(B) *B. abortus* 2308 CFU counts in $CD11b^-$ and $CD11b^+$ splenocytes from C57BL/6J mice (n = 5) at 9 and 30 days postinfection (dpi).

(C) Frequency *of B. abortus*-infected $CD11b^+$ dendritic cells (DCs, $F4/80^-Ly6G^-CD11b^+CD11c^+$), $Ly6C^{high}$ macrophages ($CD11c^-Ly6G^-CD11b^+F4/80^+Ly6C^{high}$), and $Ly6C^{low}$ macrophages ($CD11c^-Ly6G^-CD11b^+F4/80^+Ly6C^{low}$) determined by flow cytometry in $CD11b^+$ splenocytes from infected C57BL/6J mice (n = 5) at 9 and 30 dpi.

(D) Representative data plot of populations shown in (C). FSC, forward scatter.

(E) Frequency of *B. abortus*-infected $CD301^+$ (AAM) and $CD301^-$ $Ly6C^{low}$ macrophages in $CD11b^+$ splenocytes determined by flow cytometry in $CD11b^+$ splenocytes from C57BL/6J infected mice (n = 5) at 30 dpi. Values represent mean ± SEM. *$p < 0.05$ and **$p < 0.01$ using one-way ANOVA for (A) or unpaired t test analysis for (B), (C), and (E).

$Ly6C^{high}$ monocytes contributed to control of *B. abortus* infection during the acute phase, since mice deficient for the C-C chemokine receptor 2 ($Ccr2^{-/-}$ mice), which are deficient for egress of $Ly6C^{high}$ monocytes from the bone marrow, were colonized ~3-fold more highly during the acute phase (9 days) of infection (Figure S1D). Macrophages from *B. abortus*-infected $Ccr2^{-/-}$ mice also had reduced levels of inflammatory markers and increased expression of AAM markers (Figure S1E), suggesting that increased numbers of AAMs in the $Ccr2^{-/-}$ mice may contribute to the increased *B. abortus* colonization observed in these mice.

In contrast to acute *B. abortus* infection, during the chronic infection phase (30 days), flow cytometric analysis of splenic macrophages ($CD3^-B220^-NK1.1^-Ly6G^-CD11b^+F4/80^+$ cells) revealed an increase in cells with a $Ly6C^{low}$ phenotype that were positive for the AAM marker CD301 (Figures 1D–1F). In addition, higher expression levels of the AAM markers *Ym1* and *Fizz1* (encoding proteins secreted by AAMs) were observed, suggesting an increased abundance of AAMs at this time point (Figure S1B). Immunohistochemical analysis of Ym1 and Fizz1 expression in splenic tissue confirmed that while these AAM markers were expressed at low levels in uninfected and acutely infected spleen tissue, the abundance of both markers was elevated during chronic infection, at day 30 (Figure S1C). Together these lines of evidence provided support for the idea that AAMs are more abundant in the spleen during the chronic infection phase of brucellosis, and suggested that AAMs may provide a niche for persistence of *B. abortus*.

AAMs Support Increased Levels of Intracellular *B. abortus* Replication

To determine whether AAMs could be a preferred niche for *B. abortus*, we quantified bacterial survival and replication in bone marrow-derived macrophages (BMDMs) that were unstimulated, treated with IFNγ to produce CAMs, or treated with interleukin-4 (IL-4) to produce AAMs (Figure 2A). As expected, BMDM responded to IL-4 with increased expression of *Ym1*, *Fizz1*, and *Il6*, while CAMs expressed higher levels of *Il6* than

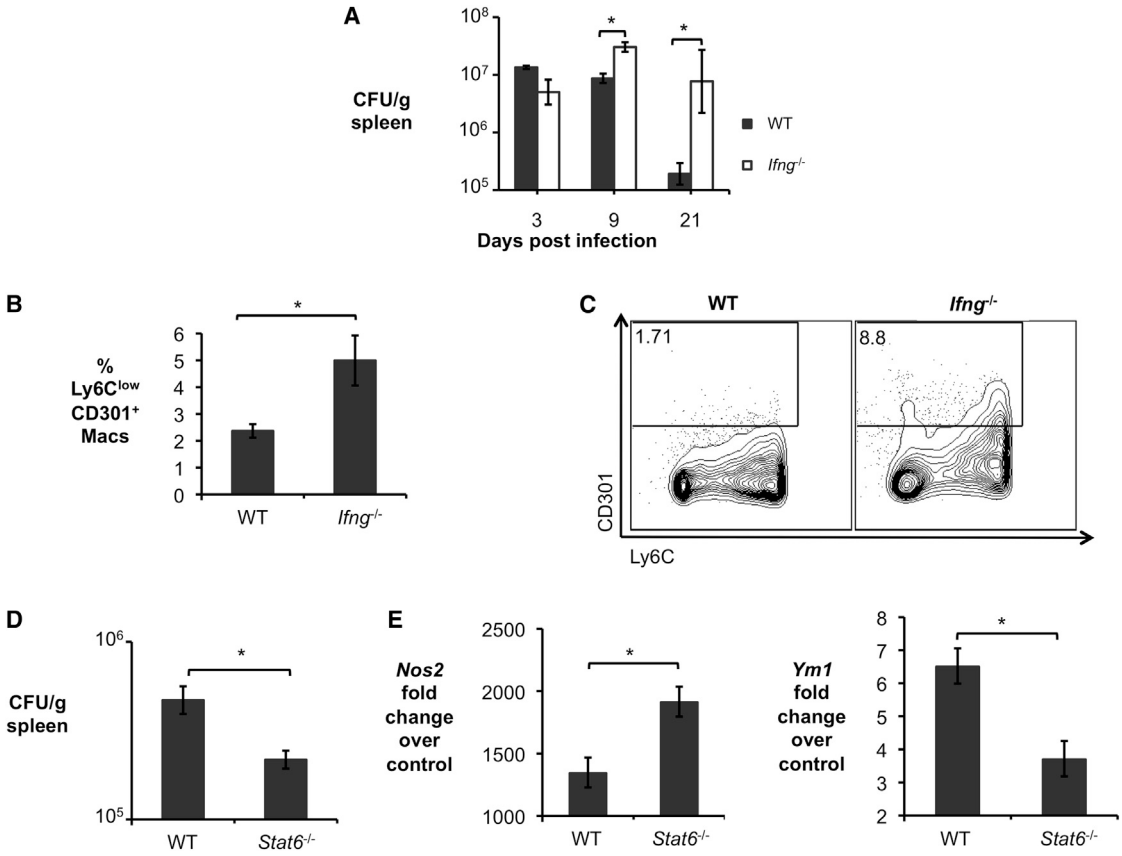

Figure 3. Defects in Generation of CAMs or AAMs Affect *B. abortus* Survival In Vivo

(A) *B. abortus* 2308 CFU counts in spleens from C57BL/6J and congenic *Ifng*$^{-/-}$ mice (n = 5) at 3, 9, and 21 days postinfection (dpi).

(B) Frequency of CD3$^-$B220$^-$NK1.1$^-$Ly6G$^-$CD11b$^+$F4/80$^+$Ly6C^{low}CD301$^+$ macrophages (AAM) measured by flow cytometry in spleens of *B. abortus*-infected C57BL/6J and congenic *Ifng*$^{-/-}$ mice (n = 5) at 9 dpi.

(C) Representative data plot of populations shown in (B).

(D) *B. abortus* 2308 CFU counts in spleens of C57BL/6J and congenic *Stat6*$^{-/-}$ mice (n = 5) at 30 dpi.

(E) Real-time RT-PCR gene expression analysis of CAM gene *Nos2* and AAM gene *Ym1* in CD11b$^+$ splenocytes from *B. abortus*-infected C57BL/6J and congenic *Stat6*$^{-/-}$ mice (n = 5) at 30 dpi. Values represent mean ± SEM. *$p < 0.05$ using unpaired t test statistical analysis. See also Figure S2.

AAMs (data not shown). While the CAMs eliminated intracellular *B. abortus* infection, both unstimulated BMDM and AAMs were permissive for intracellular replication of *B. abortus* (Figure 2A). Remarkably, *B. abortus* replicated to 10-fold higher numbers in AAMs than in untreated control BMDMs, demonstrating an increased capacity of these cells to support intracellular infection (Figure 2A).

To determine whether the AAMs also serve as a preferential niche for *B. abortus* during chronic infection, we determined the intracellular localization of *B. abortus* by enrichment of CD11b$^+$ cells and flow cytometry (Figure 2). During the acute infection, *B. abortus* was recovered from both the CD11b$^+$ and the CD11b$^-$ cell fraction, consistent with a previous report (Copin et al., 2012). However, during chronic infection, *B. abortus* localized predominantly to the CD11b$^+$ fraction (Figure 2B). Flow cytometric analysis of the CD11b$^+$ fraction revealed that that during acute infection *B. abortus* localized to CD11b+ dendritic cells, as well as to macrophages that were Ly6C^{high} and Ly6C^{low} (Figures 2C and 2D). In contrast, during chronic infection, *B. abortus* colocalized with macrophages that were Ly6C^{low}. Since AAMs are described to express low levels of Ly6C as well as the marker CD301, we further analyzed the Ly6C^{low} population for expression of CD301 and found an approximately 5-fold higher association of *B. abortus* with Ly6C^{low} CD301$^+$ cells (AAMs) than with Ly6C^{low} CD301$^-$ cells (Figure 2E). Together, these results demonstrated that *B. abortus* preferentially associated with AAMs during chronic (but not acute) infection.

Since the results shown above suggested that AAMs could be a niche for intracellular persistence of *B. abortus*, we tested whether mice with defects in generation of CAMs (*Ifng*$^{-/-}$ mice) or AAMs (*Stat6*$^{-/-}$ mice) would be altered in their ability to control *B. abortus* infection (Figure 3). Consistent with findings of other groups, *Ifng*$^{-/-}$ mice were severely deficient in control of *B. abortus* infection during the acute phase, where bacterial numbers increased rapidly (Figure 3A). This increased load of *B. abortus* correlated with an increase in the number of Ly6C^{low} CD301$^+$ AAMs (Figures 3B and 3C). Compared to control (C57BL/6) mice, *Ifng*$^{-/-}$ mice expressed lower levels of the CAM markers *Il6* and *Nos2* and higher levels of the AAM marker

Ym1 in splenic macrophages during the acute infection phase (Figure S2D). Moreover, immunohistochemical analysis confirmed increased levels of the AAM markers Ym1 and Fizz1 in spleens of *Ifng*$^{-/-}$ mice during acute infection (days 9 and 21) when compared to control mice (Figure S2E, data not shown). These results suggested that IFNγ deficiency resulted in an increase in numbers of AAMs during the acute phase of *B. abortus* infection. Thus, one important role of IFNγ in controlling *B. abortus* during the acute phase of infection may be to direct the differentiation of CAMs. The opposite effect was seen in *Stat6*$^{-/-}$ mice, which demonstrated an increased ability to control *B. abortus* persistence during the chronic infection phase (30 dpi; Figure 3D). Increased control of *B. abortus* in these mice correlated with decreased expression of AAM markers and increased CAM marker expression in splenic macrophages, suggesting that a decrease in AAM polarization in the *Stat6*$^{-/-}$ mice contributes to their increased resistance to *B. abortus* infection (Figure 3E).

PPARγ Promotes Intracellular *B. abortus* Replication in AAMs

A pathway that is crucial to acquisition and maintenance of the AAM phenotype is mediated by PPARs, a family of nuclear receptors that regulate transcription of genes involved in cellular metabolism (Odegaard et al., 2007; Vats et al., 2006). Since our previous studies of *B. abortus* genes involved in persistent but not acute infection implicated metabolic genes in this process (Hong et al., 2000), we tested the hypothesis that PPAR-mediated changes to macrophage metabolism could provide an environment for intracellular persistence of *B. abortus*. To determine whether any of the PPARs could be involved in this process, we analyzed transcripts of the PPARs in splenic CD11b^{+} cells. Our results showed that transcription of *Pparg*, the gene encoding PPARγ, was reduced during acute infection compared to uninfected controls, while during chronic infection (30–60 days) it was elevated (Figure 4A). Moreover, *Ifng*$^{-/-}$ mice had increased *Pparg* expression in splenic macrophages during acute infection, while the opposite was true for chronically infected *Stat6*$^{-/-}$ mice when compared to control animals (data not shown). In *B. abortus*-infected mice, blocking of PPARγ activity by treating the mice with the inhibitor GW9662 specifically prior to chronic infection (days 18–30) led to a significant decrease in splenic colonization at 30 days after infection, suggesting that pathways downstream of PPARγ contribute to generating a niche for persistence of *B. abortus* (Figure 4B). Concomitantly, PPARγ inhibition led to a reduction in the proportion of Ly6C^{low} CD301^{+} AAMs in the spleen at 30 dpi (Figure 4C), as well as to decreased expression of the AAM marker *Ym1* and to increased expression levels of CAM gene *Nos2* and in splenic CD11b^{+} cells (Figure S3A). These results suggested that inhibition of PPARγ reduced *B. abortus* survival by reducing the abundance of AAMs during chronic infection (Figure 4C).

Conversely, treatment of *B. abortus*-infected mice with the PPARγ agonist Rosiglitazone led to a small (2-fold) increase in *B. abortus* colonization during the acute (9 day) phase and an ~4-fold increase during the chronic (30 day) infection phase (Figure 4D). During the acute infection phase, Rosiglitazone treatment led to an increased percentage of Ly6C^{low}CD301^{+} macrophages (Figure 4E), as well as a shift toward expression of AAM markers and a reduction in the CAM marker *Nos2* (Figure S3B), suggesting that the increase in *B. abortus* infection in Rosiglitazone-treated mice resulted from a relative increase in AAMs during the acute phase of infection. Since systemic modulation of PPARγ activity could have effects on cells other than macrophages, we repeated these treatments on in vitro polarized AAMs. Similar to what we observed in vivo, *Pparg* was strongly induced in AAMs differentiated in vitro (Figure 4F). Inhibition of PPARγ activity in AAMs with GW9662 resulted in a decreased ability to support intracellular replication of *B. abortus*, while activation of PPARγ led to an additional increase in *B. abortus* replication (Figure 4G). Moreover, fluorescence microscopy analysis confirmed that increased *B. abortus* CFU counts in AAMs and PPARγ-stimulated macrophages were due to increased bacterial numbers within each cell, rather than a higher number of infected cells (Figure S3C). Together, these results suggest that PPARγ-dependent modulation of macrophage physiology promotes intracellular persistence of *B. abortus*.

PPARγ Increases the Availability of Intracellular Glucose in AAMs

One of the metabolic changes mediated by PPARγ is a shift from oxidative metabolism of glucose to β-oxidation of fatty acids. Further, PPARγ agonists are used therapeutically to lower blood glucose by increasing cellular glucose uptake (Yki-Järvinen, 2004). Since *B. abortus* is able to utilize glucose for growth (McCullough and Beal, 1951), we tested the possibility that increased intracellular glucose availability could promote intracellular replication of *B. abortus* in AAMs.

We first investigated whether *B. abortus* infection altered the phenotype of macrophages cultured in vitro. Infection of nonpolarized macrophages with *B. abortus* or the closely related *B. melitensis* led to moderately increased abundance of glycolytic pathway enzymes (Figure S4A), as well as an increase in expression of the CAM markers *Hifa*, *Pfkfb3*, and *Glut1* (Figure S4B). In contrast, *B. abortus* infection decreased expression of *Pgc1b*, encoding a transcriptional activator and of *Acadm* and *Acadl*, encoding enzymes involved in mitochondrial β-oxidation (Figure S4C). The induction of the glycolytic pathway in *B. abortus*-infected macrophages was confirmed by detection of increased concentrations of extracellular lactate, an end product of glycolysis (Figure S4D). The relative induction of the macrophage glycolytic pathway by *B. abortus* was dependent on the macrophage phenotype: infection of CAMs (induced by IFNγ) or AAMs (induced by IL-4) treated with the PPARγ antagonist GW9662 shifted the metabolism more strongly toward glycolysis and led to a marked reduction in β-oxidation genes expression (Figures 5A–5C). In contrast, compared to control (untreated) macrophages, the shift toward glycolysis induced by *B. abortus* infection was attenuated in AAMs or in cells treated with Rosiglitazone (Figures 5A–5C). Taken together, these data suggested that while *B. abortus* infection does not induce AAM polarization, infection of AAMs results in lower induction of the glycolytic pathway in the infected macrophages.

Compared to untreated control BMDMs, AAMs induced in vitro by IL-4 treatment had significantly elevated glucose content, which was lowered to the level of control macrophages by infection with *B. abortus*, raising the possibility that the pathogen

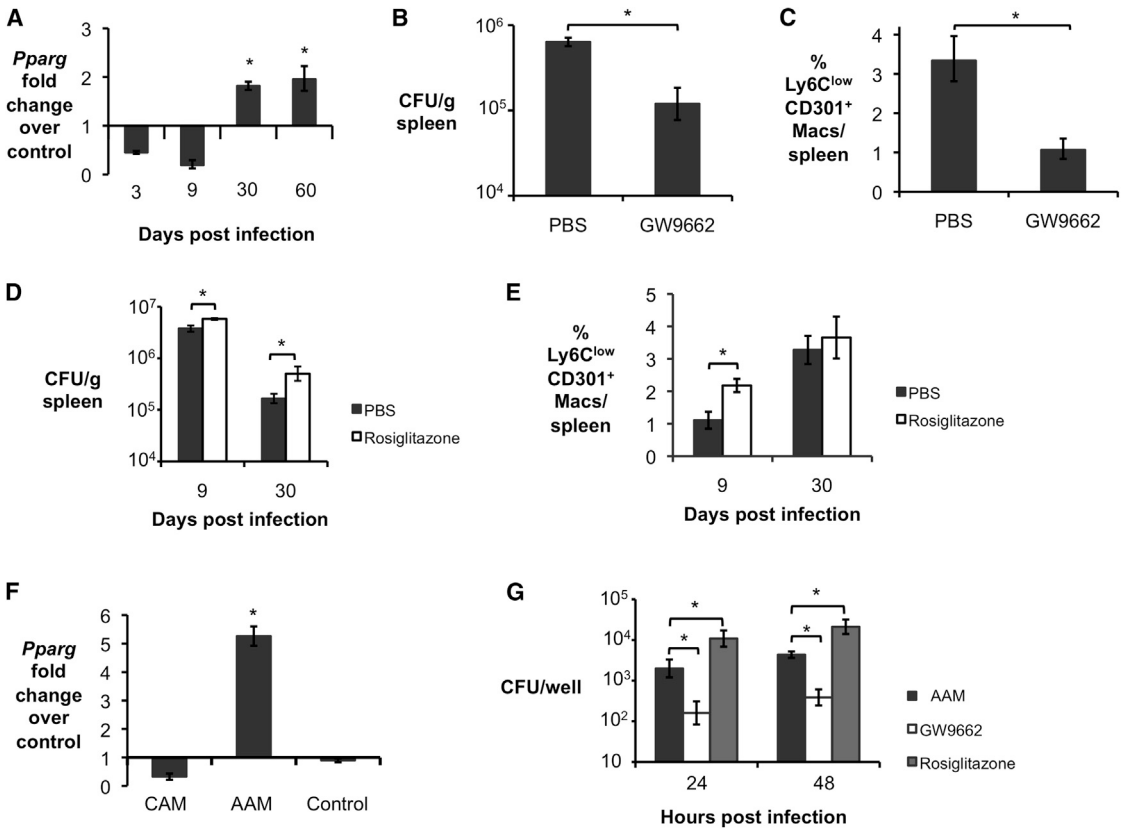

Figure 4. Increased Survival of *B. abortus* during Chronic Infection Is Dependent on PPARγ

(A) Real-time RT-PCR gene expression analysis of *Pparg* in CD11b$^+$ splenocytes from *B. abortus*-infected C57BL/6J mice (n = 5) at 3, 9, 30, and 60 dpi.

(B) *B. abortus* 2308 CFU counts, measured at 30 dpi, in spleens from C57BL/6J mice (n = 5) treated daily from 18 to 30 dpi with PPARγ antagonist GW9662 or PBS control.

(C) Frequency of CD3$^-$B220$^-$NK1.1$^-$Ly6G$^-$CD11b$^+$F4/80$^+$Ly6C^{low}CD301$^+$ macrophages (AAM) measured by flow cytometry at 30 dpi in spleens of C57BL/6J mice (n = 5) treated daily from 18 to 30 dpi with PPARγ antagonist GW9662 or PBS control.

(D) *B. abortus* 2308 CFU counts, measured at 9 and 30 dpi, in spleens from C57BL/6J mice (n = 5) treated daily for 7 days prior to infection with PPARγ agonist Rosiglitazone or PBS control.

(E) Frequency of CD3$^-$B220$^-$NK1.1$^-$Ly6G$^-$CD11b$^+$F4/80$^+$Ly6C^{low}CD301$^+$ macrophages (AAM) measured by flow cytometry at 9 and 30 dpi in spleens from C57BL/6J mice (n = 5) treated daily for 7 days prior to infection with PPARγ agonist Rosiglitazone or PBS control.

(F) Real-time RT-PCR gene expression analysis of *Pparg* in BMDMs from C57BL/6J mice stimulated with rIFN-γ (CAM) or rIL-4 (AAM), or nonstimulated (Control), and infected with *B. abortus* for 24 hr. Data shown are compiled from four independent experiments.

(G) *B. abortus* 2308 CFU counts in BMDMs from C57BL/6J mice, stimulated with rIL-4 (AAM) or with IL-4 + 3 μM of PPARγ antagonist GW9662 (GW9662) or with 5 μM of PPARγ agonist Rosiglitazone and infected with *B. abortus* for 24 and 48 hr. Data shown in (F) and (G) are compiled from four independent experiments. Values represent mean ± SEM. *p < 0.05 using one way ANOVA for (A) and (F) or unpaired t test analysis for (B)–(E) and (G). See also Figure S3.

may consume this carbon source (Figure 5D). Increased intracellular glucose in AAMs was recapitulated by treatment with Rosiglitazone, and was negated by treatment of AAMs with GW9662, suggesting that increased intracellular glucose in AAMs is dependent on PPARγ-mediated transcriptional changes (Figure 5D). Interestingly, our previous work identified a glucose transporter of the major facilitator superfamily, GluP, as a *B. abortus* factor required for chronic, but not acute, infection (Essenberg et al., 1997; Hong et al., 2000).

To directly test the idea that glucose availability could promote intracellular replication of *B. abortus* in AAMs, we compared replication of wild-type *B. abortus* and the *gluP* mutant. In vitro, the *gluP* mutant grew similarly to wild-type *B. abortus* in medium (Tryptone/Soytone) lacking glucose, while addition of glucose enhanced replication of wild-type *B. abortus*, but not of the *gluP* mutant (Figure S5A). Enhanced growth in glucose-containing medium was restored by complementation of the *gluP* mutation (Figure S5A). Remarkably, while there was no difference in the ability of the two *B. abortus* strains to survive in untreated control macrophages, wild-type *B. abortus* was recovered in 10-fold greater numbers than the *gluP* mutant from AAMs (Figure 6A). Treatment of unpolarized BMDM with Rosiglitazone increased the intracellular replication of wild-type *B. abortus* but had no effect on intracellular replication of the *gluP* mutant, consistent with an inability to utilize increased glucose within the macrophage (Figure 6B). The growth advantage of wild-type *B. abortus* over the *gluP* mutant was eliminated by treatment of AAMs with GW9662 (Figure 6B). Inhibition of mitochondrial β-oxidation in AAMs or Rosiglitazone-treated cells, using the carnitine palmitoyltransferase inhibitor etomoxir,

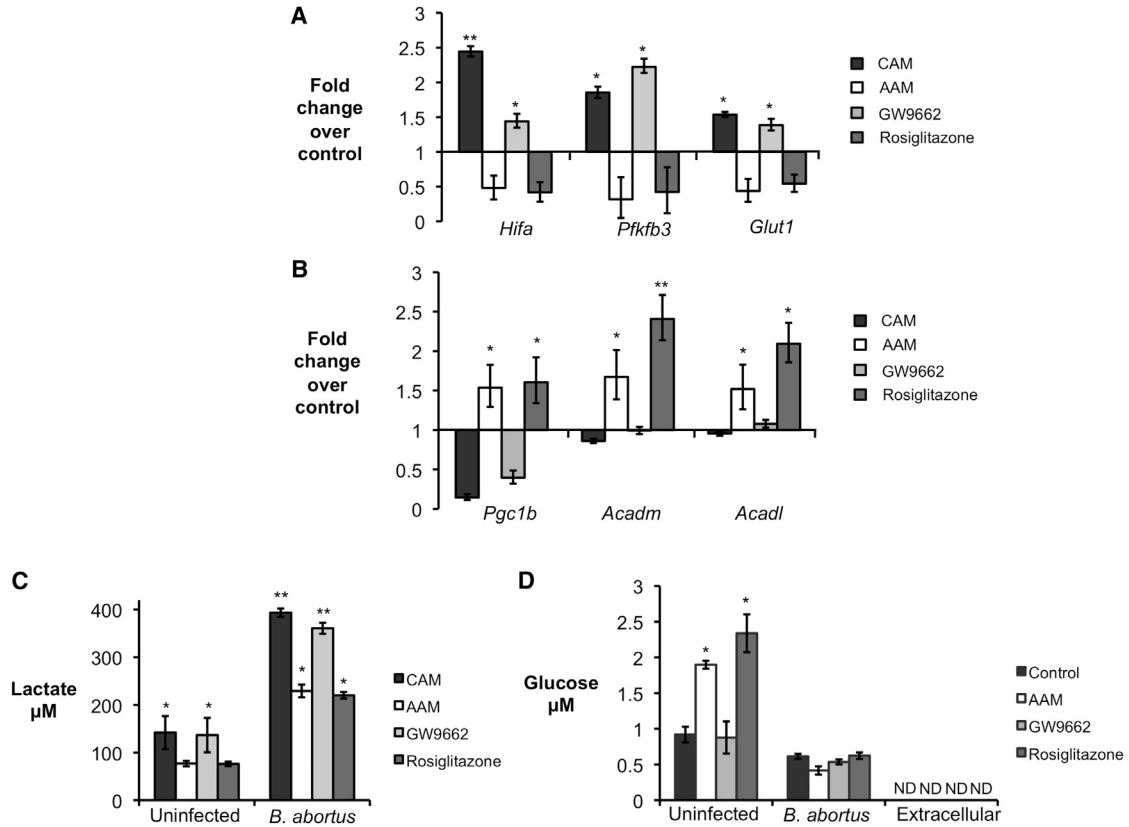

Figure 5. *B. abortus*-Infected AAMs Exhibit a PPARγ-Dependent Decrease in Glycolytic Metabolism

(A) Real-time RT-PCR gene expression analysis of glycolytic pathway genes *Hifa* (hypoxia-inducible factor α), *Pfkfb3* (phosphofructokinase-3), and *Glut1* (glucose transporter 1) in C57BL/6J BMDM stimulated with rIFNγ (CAM), with rIL-4 (AAM), with IL-4 + GW9662 (GW9662), or with Rosiglitazone and infected with *B. abortus* for 8 hr. Results are expressed as fold change over untreated macrophages infected with *B. abortus*.

(B) Real-time RT-PCR gene expression analysis of fatty acid β-oxidation pathway genes *Pgc1b* (PPARγ coactivator 1 β), *Acadm* (medium-chain acyl-CoA dehydrogenase), and *Acadl* (long-chain acyl-CoA dehydrogenase) in BMDMs from C57BL/6J stimulated rIFNγ (CAM), with rIL-4 (AAM), with IL-4 + GW9662 (GW9662), or with Rosiglitazone and infected with *B. abortus* for 8 hr. Results are expressed as fold change over untreated macrophages infected with *B. abortus*.

(C) Measurement of lactate concentration in supernatant from BMDM from C57BL/6J stimulated with rIFNγ (CAM), with rIL-4 (AAM) or IL-4 + GW9662 (GW9662), or with Rosiglitazone and uninfected or infected with *B. abortus* for 24 hr.

(D) Measurement of intracellular glucose concentration in BMDMs from C57BL/6J unstimulated (control) and stimulated with rIL-4 (AAM), with IL-4 + GW9662 (GW9662), or with Rosiglitazone and uninfected or infected with *B. abortus* for 24 hr. Values represent mean ± SEM and represent combined results of four independent experiments conducted in duplicate. *$p < 0.05$ and **$p < 0.01$ using one-way ANOVA. See also Figure S4.

also reduced the ability of *B. abortus* to replicate intracellularly, but had no effect on the *gluP* mutant (Figure 6C and Figure S5B). The growth defect of the *gluP* mutant within AAMs or Rosiglitazone-treated macrophages was restored by complementation (Figures 6D and 6E), demonstrating that the ability to transport glucose is essential for increased growth in these macrophages. To control for possible off-target effects of the inhibitors on *B. abortus*, we examined replication of wild-type and the *gluP* mutant in macrophages from conditionally PPARγ-deficient mice, in which only macrophages lack PPARγ (Figures S5C and S5D). Similarly to what was observed with the PPARγ inhibitor-treated AAMs (Figure 6B), GluP-dependent replication of *B. abortus* within either IL-4 or Rosiglitazone-treated macrophages was dependent on the function of PPARγ (Figures S5C and S5D). These results provide evidence that the increased replication of *B. abortus* in AAMs is dependent on its ability to utilize the elevated intracellular pool of glucose that is induced by PPARγ.

Persistent Infection by *B. abortus* Depends on the Ability to Transport Glucose

The results presented above raised the question of whether the PPARγ-dependent increase in glucose concentration that we observed in cultured macrophages could also promote *B. abortus* infection in vivo. To investigate this, we determined the requirement for GluP during acute and chronic infection (Figure 7A), using a competitive infection assay. During acute infection (9 days), the ratio of wild-type *B. abortus* to the *gluP* mutant was not significantly different from the 1:1 ratio in the inoculum (Figure 7A). However, during chronic infection, the *gluP* mutant was outcompeted 20-fold by the wild-type. To determine whether this competitive defect was the result of PPARγ activation, we repeated the experiment in mice treated with the PPARγ antagonist GW9662 (Figure 7B). Inhibition of PPARγ during the chronic infection stage strongly reduced the competitive defect of the *gluP* mutant at 30 dpi. Since the survival defect of the *gluP* mutant was observed only during chronic infection, when PPARγ

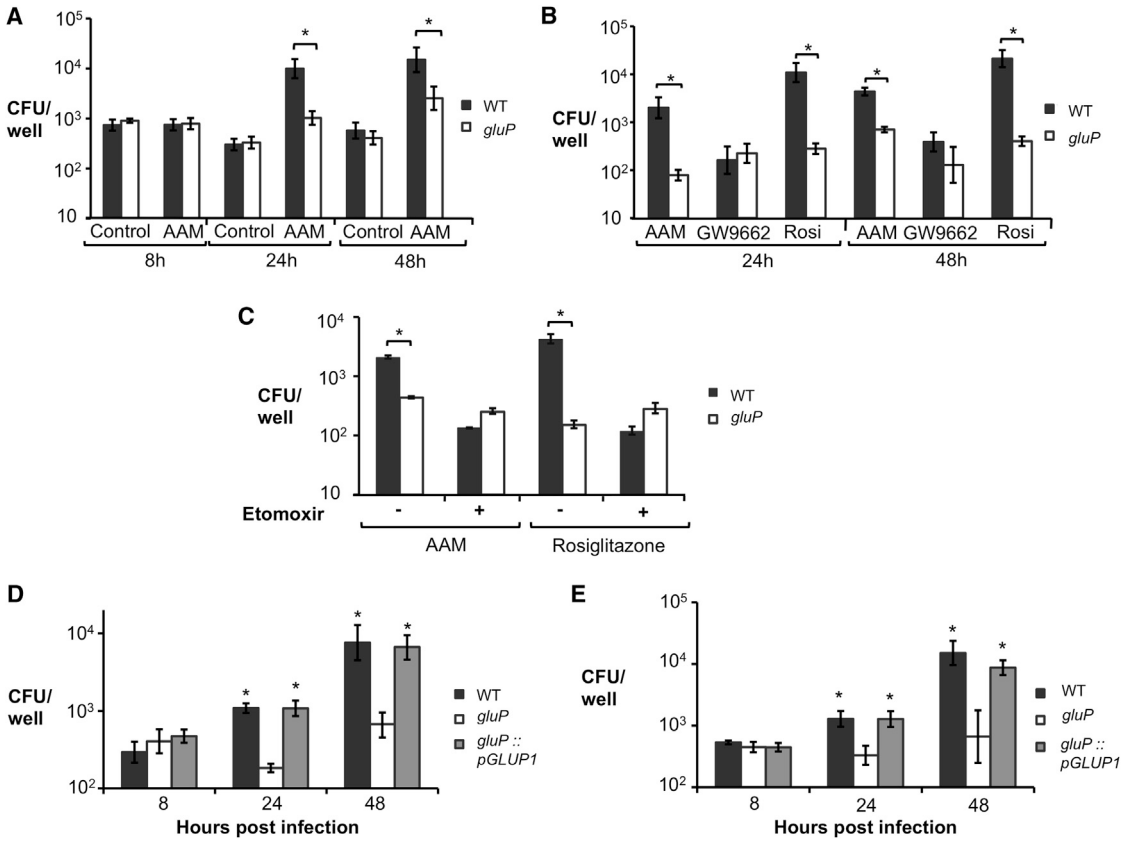

Figure 6. A PPARγ-Dependent Increase in Intracellular Glucose Availability Promotes Survival of *B. abortus* in Macrophages

(A) Recovery of *B. abortus* from C57BL/6J BMDM that were sham treated (Control) or treated with rIL-4 (AAM). BMDM were infected with *B. abortus* 2308 WT or isogenic *gluP* mutant for 8, 24, and 48 hr.

(B) Recovery of *B. abortus* from C57BL/6J BMDM stimulated with rIL-4 (AAM), with IL-4 + GW9662 (GW9662), or with Rosiglitazone (Rosi) and infected with *B. abortus* 2308 (WT) or isogenic *gluP* mutant for 24 and 48 hr.

(C) Recovery of *B. abortus* from BMDMs from C57BL/6J treated or not with the β-oxidation inhibitor etomoxir (50 μM) in the presence of rIL-4 (AAM) or Rosiglitazone and infected with *B. abortus* 2308 WT or isogenic *gluP* mutant for 48 hr.

(D) Recovery of *B. abortus* from BMDMs from C57BL/6J stimulated rIL-4 (AAM) and infected with *B. abortus* 2308 WT or isogenic *gluP* mutant or complemented *gluP* mutant (*gluP*::pGLUP1) for 8, 24, and 48 hr.

(E) Recovery of *B. abortus* from BMDMs from C57BL/6J stimulated with Rosiglitazone and infected with *B. abortus* 2308 WT or isogenic *gluP* mutant or complemented *gluP* mutant (*gluP*::pGLUP1) for 8, 24, and 48 hr. Values represent mean ± SEM of data from four independent experiments conducted in duplicate. *$p < 0.05$ using unpaired t test for (A)–(C) or one-way ANOVA statistical analysis for (D) and (E). See also Figure S5.

expression was increased, we next asked whether activation of PPARγ during acute infection would affect the survival of the *gluP* mutant (Figure 7C). Treatment of mice during acute infection with Rosiglitazone increased the ability of the wild-type *B. abortus* to outcompete the *gluP* mutant at 9d by approximately 4-fold, resembling the phenotype only previously seen at later stages of infection (30 days). Finally, to control for off-target effects of the inhibitors, we repeated the competitive infection in mice conditionally deficient for *Pparg* expression in macrophages (*Pparg*$^{flox/flox}$ LysM$^{cre/-}$; Odegaard et al., 2007). The growth advantage of wild-type *B. abortus* over the *gluP* mutant was strongly reduced in the conditionally *Pparg*-deficient mice (Figure 7D), demonstrating that expression of PPARγ specifically in macrophages is required for *B. abortus* to benefit from acquisition of glucose in AAMs during chronic infection. Taken together, these results demonstrate that, in vivo, the ability of *B. abortus* to benefit from PPARγ-mediated changes in host macrophage metabolism is dependent on the ability of *B. abortus* to take up glucose.

DISCUSSION

Recent studies have shed light on the extensive interactions between immune and metabolic functions of macrophages. For the case of CAMs, oxygen is required as a substrate for NADPH oxidase, and therefore these cells meet their energetic needs via anaerobic glycolysis. Since anaerobic glucose utilization is a relatively inefficient way to generate ATP (only 2 ATP/molecule of glucose), a large amount of glucose must be utilized, and the relative intracellular concentration of free glucose is low. In contrast, in AAMs, this metabolic program is antagonized by STAT6-dependent induction of PPARγ and PPARδ (Szanto et al., 2010). As a result, AAMs shift to aerobic metabolism, in which they gain energy by β-oxidation of fatty acids (Bensinger

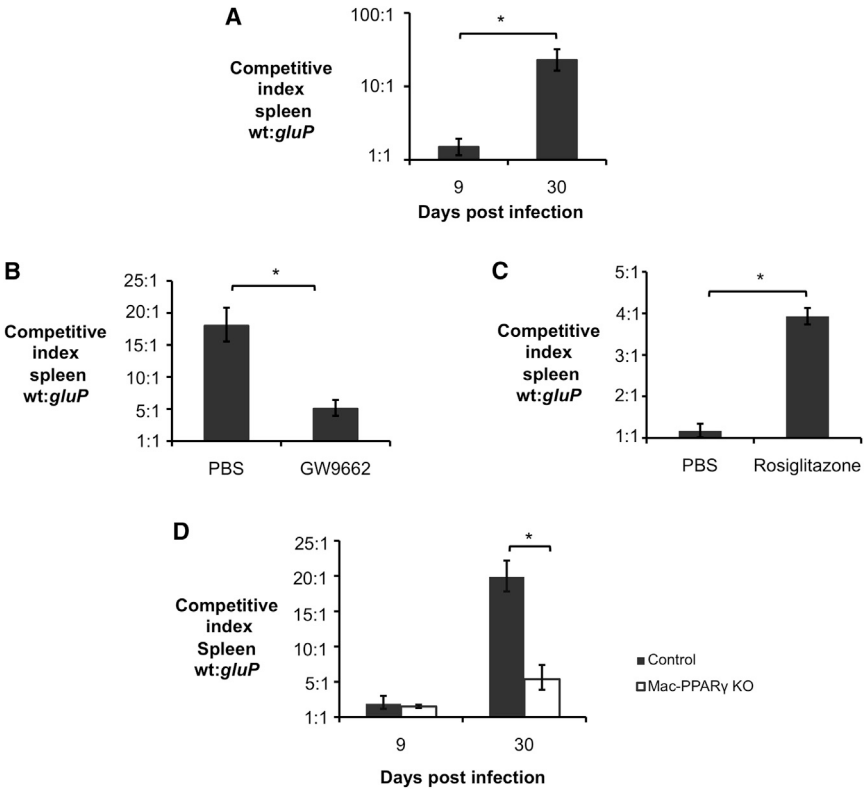

Figure 7. A PPARγ-Dependent Increase in Intracellular Glucose Availability in Macrophages Promotes *B. abortus* Persistence In Vivo

(A) Competitive index (ratio of WT to *gluP* mutant) in spleens of C57BL/6J mice (n = 5) infected with a 1:1 mixture of *B. abortus* 2308 WT and isogenic *gluP* mutant for 9 and 30 days.

(B) Competitive index, measured at 30 days postinfection (dpi), in spleens from C57BL/6J mice (n = 5) treated daily from 18 to 30 dpi with PPARγ antagonist GW9662 or PBS control and infected with a 1:1 mixture of *B. abortus* 2308 WT and isogenic *gluP* mutant.

(C) Competitive index, measured at 9 and 30 dpi, in spleens from C57BL/6J mice (n = 5) treated daily for 7 days prior to infection with PPARγ agonist Rosiglitazone or PBS control and infected with a 1:1 mixture of *B. abortus* 2308 WT and isogenic *gluP* mutant.

(D) Competitive index, measured at 9 and 30 dpi, in spleens from $Pparg^{fl/fl}LysM^{cre/-}$ (Mac-PPARγ KO) or littermates $Pparg^{fl/fl}LysM^{-/-}$ (Control) mice (n = 5) infected with a 1:1 mixture of *B. abortus* 2308 WT and isogenic *gluP* mutant. Values represent mean ± SEM. *$p < 0.05$ using unpaired t test statistical analysis.

and Tontonoz, 2008; O'Neill and Hardie, 2013). Our results demonstrate that this metabolic shift leads to an increase in intracellular glucose, which becomes available to support growth of intracellular bacteria (Figure 5). An exhaustive screen of *B. suis* genes required for intracellular infection in human THP-1 cells identified sugar metabolism genes as being required for intracellular infection and suggested that the replicative niche for *Brucella* within the cell is poor in nutrients (Kohler et al., 2002). Further, at late stages during cellular infection, the bacterial glycolysis pathway was downregulated, which led to the proposition that *Brucella* may use fatty acids or amino acids rather than sugars during this growth phase (Al Dahouk et al., 2008; Barbier et al., 2011). However, the increased growth rate of *B. abortus* within AAMs in vitro compared to unpolarized or CAM-polarized macrophage populations used for previous studies suggests that AAMs may provide additional nutrients, such as glucose, that are less abundant in other macrophage populations.

Like *B. abortus*, other bacteria have been shown to induce PPARγ expression, such as *Mycobacterium tuberculosis* (Mahajan et al., 2012) and *Listeria monocytogenes* (Abdullah et al., 2012). Interestingly, a lack of PPARγ expression in macrophages was shown to render mice more resistant to *L. monocytogenes* infection (Abdullah et al., 2012). While the underlying mechanism in this study was not identified, our work shows that antagonizing PPARγ activity during *B. abortus* infection helps control the pathogen burden by reducing intracellular glucose availability. Importantly, these observations, together with findings by Eisele et al. (2013; in this issue) demonstrating that PPARδ-dependent modulation of glucose concentration stimulates intracellular growth of *Salmonella enterica* serotype Typhimurium in AAM, raise the possibility that PPAR-induced increases in intracellular glucose availability may be a general mechanism promoting growth of persistent pathogens within AAMs.

It should be noted that unlike *Francisella tularensis*, which induces differentiation of AAMs to promote its replication (Shirey et al., 2008), *B. abortus* does not appear to induce this pathway directly, since cultivation of *B. abortus* with BMDM in vitro did not induce expression of AAM markers (Figure S4). Rather, as a result of its inherently low TLR4-stimulatory activity for macrophages and dendritic cells (reviewed by Martirosyan et al., 2011), *B. abortus* induces only a weak and transient Th1 response during the acute infection phase, which is characterized by an influx of inflammatory macrophages (Figure 1, Figure S2A; and Copin et al., 2012). It is likely that this transient IFNγ response is unable to sustain the CAM polarization of these cells, and perhaps together with the constant IL-4 levels throughout infection (Figure S2B) as well as induction of IL-13 (Figure S2C) and PPARγ during chronic infection by *B. abortus*, macrophages that have already entered the site of infection may become polarized to the AAM phenotype. Such a scenario would be consistent with our finding of similar increases in macrophage numbers during both acute and chronic infection but a relative increase in AAMs only during the chronic infection phase. These findings in the mouse model are consistent with reports of transient IFNγ responses and an increase in IL-13 producing T cells in human patients with chronic brucellosis (Rafiei et al., 2006).

Our results fit with previous reports suggesting that, during chronic infection, persistent pathogens undergo a shift in their metabolism. For example, it has long been known that

M. tuberculosis utilizes the glyoxylate shunt during intracellular infection (Wayne and Lin, 1982), and characterization of isocitrate lyase, an enzyme of this pathway needed for the chronic, but not the acute phase of infection (McKinney et al., 2000), identified this enzyme as a potential therapeutic target. Like tuberculosis, brucellosis is a chronic infection causing significant morbidity that requires protracted treatment with multiple antibiotics. Treatment failures and relapses are common for brucellosis; therefore identification of PPARγ, a well-characterized drug target, as a host factor providing a metabolic advantage to *B. abortus* during chronic infection suggests inhibitors of PPARγ as a potential adjunct to antibiotic therapy for the prevention of relapsing chronic infection.

EXPERIMENTAL PROCEDURES

Bacterial Strains, Media, and Culture Conditions

Bacterial strains used in this study were the virulent strain *Brucella abortus* 2308; its isogenic mutant strain MX2, which has an insertion of pKSoriT-*bla-kan*-P*sojA-mCherry* plasmid (Copin et al., 2012); BA159 (*gluP*), which has a miniTn*5* Km2 transposon insertion interrupting the *gluP* locus (Hong et al., 2000); and the complemented *gluP* mutant MX6 (*gluP*::pGLUP1). For construction of strain MX6, the *gluP* gene sequence including its promoter was amplified by PCR using the primers GluP FWD, 5′- GTCGACTTTGTTGGCTTTCAAGTGG-3′; and GluP REV, 5′-GGATCCTCGCCATTCTATTCGGTTTC-3′. The resulting *gluP* PCR product was cloned into pCR2.1 using the TOPO TA cloning kit (Invitrogen, Carlsbad) and correct insertion confirmed by sequencing (SeqWright Fisher Scientific, Houston) and plasmid digestion using enzymes SalI and BamHI. The final construct (pGLUP1) was introduced by electroporation to strain BA159 to reconstitute the intact gene. For strain MX6, positive clones were selected based on ampicillin (Amp) resistance, and intact gene chromosomal insertion was further confirmed by PCR. For strain MX2, positive clones were kanamycin (Km) resistant and fluorescent, as previously described (Copin et al., 2012). Strains were cultured on tryptic soy agar (Difco/Becton Dickinson, Sparks, MD) or tryptic soy broth at 37°C on a rotary shaker. Bacterial inocula for mouse infection were cultured on tryptic soy agar plus 5% blood for 3 days (Alton et al., 1975). For cultures of strain MX2 and BA159, Km was added to the culture medium at 100 μg/mL. All work with *B. abortus* cells was performed at biosafety level 3 and was approved by the Institutional Biosafety Committee at the University of California, Davis.

Animal Experiments

Female C57BL/6J wild-type mice, *Ifng*$^{-/-}$ mice, *Ccr2*$^{-/-}$ mice, and *Stat6*$^{-/-}$ mice, aged 6–8 weeks, were obtained from The Jackson Laboratory (Bar Harbor). Female and male C57BL/6 *Pparg*$^{fl/fl}$*LysM*$^{cre/-}$ (Mac-PPARγ KO) and littermate *Pparg*$^{fl/fl}$*LysM*$^{-/-}$ (control) mice were generated at UC Davis by mating *Pparg*$^{fl/fl}$ mice with LysM$^{cre/cre}$ mice (The Jackson Laboratory, Bar Harbor). Mice were held in microisolator cages with sterile bedding and irradiated feed in a biosafety level 3 laboratory. Groups of four to six mice were inoculated intraperitoneally (i.p.) with 0.2 ml of phosphate-buffered saline (PBS) containing 5 × 10^5 CFU of *B. abortus* 2308 or a 1:1 mixture of *B. abortus* 2308 and *gluP* mutant as previously described (Rolán and Tsolis, 2008). At 0, 3, 9, 15, 21, 30, and/or 60 days after infection, according to the experiment performed, the mice were euthanized by CO_2, and their spleens were collected aseptically at necropsy. The spleens were homogenized in 2 ml of PBS, and serial dilutions of the homogenate were plated on TSA and/or TSA+ kanamycin for enumeration of CFU. Spleen samples were also collected for gene expression, flow cytometry, and immunohistochemistry analysis as described below. All animal experiments were approved by the University of California Laboratory Animal Care and Use Committee and were conducted in accordance with institutional guidelines.

Bone Marrow-Derived Macrophage Infection

BMDMs were differentiated from bone marrow precursors from femora and tibiae of female, 6- to 8-week-old, C57BL/6J mice or Mac-PPARγ KO (*Pparg*$^{-/-}$) and littermate control (WT) mice following a previously published procedure (Rolán and Tsolis, 2007). For BMDM experiments, 24-well microtiter plates were seeded with macrophages at concentration of 5 × 10^5 cells/well in 0.5 ml of RPMI media (Invitrogen, Grand Island, NY) supplemented with 10% FBS and 10 mM L-glutamine (RPMI supl) incubated for 48 hr at 37°C in 5% CO_2. Preparation of the inoculum and BMDM infection was performed as previously described (Rolán and Tsolis, 2007). Briefly, for inoculum preparation, *B. abortus* 2308 or *B. abortus* BA159 (*gluP*) or MX6 was grown for 24 hr and then diluted in RPMI supl, and about 5 × 10^7 bacteria in 0.5 ml of RPMI supl was added to each well of BMDM, reaching multiplicity of infection (moi) of 100. Microtiter plates were centrifuged at 210 × *g* for 5 min at room temperature in order to synchronize infection. Cells were incubated for 20 min at 37°C in 5% CO_2, free bacteria were removed by three washes with phosphate-buffered saline (PBS), and the zero time point sample was taken as described below. After the PBS wash, RMPI supl plus 50 mg gentamicin per mL was added to the wells, and the cells were incubated at 37°C in 5% CO_2. In order to determine bacterial survival, the medium was aspirated at 0, 8, 24, and 48 hr after infection according to the experiment performed, and the BMDMs were lysed with 0.5 ml of 0.5% Tween 20, followed by rising of each well with 0.5 ml of PBS. Viable bacteria were quantified by serial dilution in sterile PBS and plating on TSA. For gene expression assays, BMDMs were resuspended in 0.5 ml of TRI-reagent (Molecular Research Center, Cincinnati) at the time points described above and kept at −80°C until further use. When necessary, 10 ng/mL of mouse rIFN-γ (BD Bioscience, San Jose, CA), 10 ng/mL of mouse rIL-4 (BD Bioscience, San Jose, CA), 3 μM of GW9662 (Cayman Ann Harbor, MI), 5 μM of Rosiglitazone (Cayman, Ann Harbor, MI), or 50 μM of Etomoxir (Sigma-Aldrich, St Louis, MO) was added to the wells overnight prior to experiment and kept throughout the experiments. All experiments were performed independently in duplicate at least four times and the standard error for each time point calculated.

CD11b$^+$ Cell Isolation

Macrophages (CD11b$^+$ cells) were isolated from the spleens of *B. abortus*-infected C57BL/6J, congenic *Ccr2*$^{-/-}$, *Ifng*$^{-/-}$, and *Stat6*$^{-/-}$ mice with a MACS CD11b MicroBeads magnetic cell sorting kit from Miltenyi Biotech (Auburn, CA) by following the manufacturer's instructions, as previously described (Rolán et al., 2009). Briefly, single-cell suspension was prepared by gently teasing apart the spleens, followed by passage of splenocytes through a 70 μm cell strainer and treatment with ACK buffer (Lonza, Walkersville, MD) to lyse red blood cells. Cells were washed with PBS-BSA, counted, and incubated with CD11b MicroBeads. Cells were applied to a magnetic column, washed, eluted, and counted. For gene expression assays, total splenic CD11b$^+$ cells per mouse were resuspended in 0.5 ml of TRI reagent (Molecular Research Center, Cincinnati) and kept at −80°C until further use. For *B. abortus* recovery essay, viable bacteria in CD11b$^-$ and CD11b$^+$ splenocytes fractions was determined by 10-fold serial dilution in sterile PBS and plating on TSA. The results were normalized to CFU per 10^6 cells.

Treatment with PPARγ Agonist/Antagonist In Vivo

Female C57BL/6J mice were inoculated intraperitoneally (i.p.), daily, for 7 days prior to *B. abortus* infection, with 5 mg/kg/day of the PPARγ agonist Rosiglitazone (Cayman, Ann Harbor, MI) diluted in 0.2 ml of sterile PBS solution. For the treatment with PPARγ antagonist GW9662 (Cayman, Ann Arbor, MI), female C57BL/6J mice were inoculated intraperitoneally (i.p.), daily, from day 18 till day 30 post-*B. abortus* infection, with 3 mg/kg/day of PPARγ antagonist GW9662 (Cayman, Ann Arbor, MI) diluted in 0.2 ml of sterile PBS solution.

RT-PCR and Real-Time PCR Analysis

Eukaryotic gene expression was determined by real-time PCR as previously described (Rolán and Tsolis, 2007). Briefly, eukaryotic RNA was isolated using TRI reagent (Molecular Research Center, Cincinnati) according to the manufacturer's instructions. A reverse transcriptase reaction was performed to prepare complementary DNA (cDNA) using TaqMan reverse transcription reagents (Applied Biosystems, Carlsbad CA). A volume of 4 μl of cDNA was used as template for each real-time PCR reaction in a total reaction volume of 25 μL. Real-time PCR was performed using SYBR Green (Applied Biosystems) along with the primers listed in Table S1. Data were analyzed using the comparative Ct method (Applied Biosystems). Transcript levels of *IL-6*,

Nos2, *Ym1*, *Fizz1*, *Tnfa*, *Pparg*, *Hifa*, *Pfkfb3*, *Glut1*, *Pgc1b*, *Acadm*, and *Acadl* were normalized to mRNA levels of the housekeeping gene *act2b*, encoding β-actin.

Flow Cytometry

Flow cytometry analysis for detection of CAMs, AAMs, and/or *B. abortus* intracellular localization was performed in splenocytes and/or CD11b$^+$ splenic cells of C57BL/6J mice infected with *B. abortus* 2308 for 9 or 30 days. Briefly, after passing the spleen cells through a 100 μm cell strainer and treating the samples with ACK buffer (Lonza, Walkersville, MD) to lyse red blood cells, splenocytes were washed with PBS (GIBCO) containing 1% bovine serum albumin (fluorescence-activated cell sorter [FACS] buffer). After cell counting, 4 × 10^6 cells/mouse were resuspended in PBS and stained with Aqua Live/Dead cell discriminator (Invitrogen, Grand Island, NY) according to the manufacturer's protocol. After Live/Dead staining, splenocytes were resuspended in 50 μl of FACS buffer, and cells were stained with cocktail of anti-B220 PE (BD Pharmigen, San Jose, CA), anti-CD3 PE (BD PharMingen), anti-NK1.1 PE (BD Pharmigen), anti-CD11b FITC (BD PharMingen), anti-F4/80 Pe.Cy7 (Biolegend, San Diego, CA), anti-Ly6C Pacific Blue (Biolegend), anti-Ly6G PerCP Cy5.5 (Biolegend), and anti-CD301 AF647 (AbD serotec, Raleigh, NC). The cells were washed with FACS buffer and fixed with 4% formaldehyde for 30 min at 4°C. To determine intracellular *B. abortus* localization in CD11b$^+$ splenocytes, cells were stained with cocktail of anti-CD11c PE (BD PharMingen), anti-CD11b FITC (BD PharMingen), anti-F4/80 Pe.Cy7 (Biolegend), anti-Ly6C Pacific Blue (Biolegend), anti-Ly6G PerCP Cy5.5 (Biolegend), and anti-CD301 AF647 (AbD Serotec), followed by cell fixation and permeabilization using Cytofix/Cytoperm (BD Pharmigen) at 4°C for 30 min. For intracellular *B. abortus* labeling, Cd11b$^+$ splenocytes were ressuspended in 50 μL of Perm/Wash buffer (BD Pharmigen) and stained with APC.Cy7 (AbD Serotec) conjugated goat anti-*B. abortus* antibody followed by two washes with Perm/Wash buffer. For all experiments, cells were ressuspended in FACS buffer prior to analysis. Flow cytometry analysis was performed using an LSRII apparatus (Becton Dickinson, San Diego, CA), and data were collected for 5 × 10^5 cells/mouse. Resulting data were analyzed using Flowjo software (Treestar, inc. Ashland, OR). Gates were based on Fluorescence-Minus-One (FMO) controls.

Lactate Measurement

For determination of extracellular lactate levels, C57BL/6J BMDM were grown in 24-well plates using RPMI media (Invitrogen, Grand Island, NY) supplemented with 2% FBS and 10 mM L-glutamine (RPMI supl) and infected as described above. At 24 hr postinfection, supernatants were collected, and lactate measurement was performed by using a Lactate Colorimetry Assay Kit (Biovision, Milpitas, CA) according to the manufacturer's instructions.

Glucose Measurement

For determination of intracellular glucose levels, C57BL/6J BMDMs were grown in 24-well plates and infected as described above. At 24 hr postinfection, cells were washed three times with cold PBS and resuspended in 100 μl of glucose assay buffer. Further glucose measurement was performed by using a Glucose Assay Kit (Biovision) according to the manufacturer's instructions.

Statistical Analysis

Fold changes of ratios (bacterial numbers or mRNA levels) and percentages (flow cytometry and fluorescence microscopy) were transformed logarithmically prior to statistical analysis. An unpaired Student's t test was used on the transformed data to determine whether differences between groups were statistically significant ($p < 0.05$). When more than two treatments were used, statistically significant differences between groups were determined by one-way ANOVA. All statistical analysis was performed using GraphPad Prism version 6b software (GraphPad Software, La Jolla, CA).

SUPPLEMENTAL INFORMATION

Supplemental Information includes five figures, one table, and Supplemental Experimental Procedures and can be found with this article online at http://dx.doi.org/10.1016/j.chom.2013.07.009.

ACKNOWLEDGMENTS

The authors are grateful to Sebastian Winter for helpful discussions during the course of this work. US PHS grants AI050553 and AI090387 to R.M.T., as well as a pilot grant from the UC Davis Proteomics Core, supported this work. T.M.A.S. was supported by a fellowship from CNPq, Brazil. We thank Xavier deBolle for providing plasmid pKSoriT-*bla-kan*-P*sojA-mCherry*. Flow cytometry was performed in a facility supported by Facilities Improvement Grant RR12088-01. The Animal Resources and Laboratory Services Core of the PSWRCE were supported by US PHS grant U54 AI065359.

Received: March 1, 2013
Revised: May 17, 2013
Accepted: June 20, 2013
Published: August 14, 2013

REFERENCES

Abdullah, Z., Geiger, S., Nino-Castro, A., Böttcher, J.P., Muraliv, E., Gaidt, M., Schildberg, F.A., Riethausen, K., Flossdorf, J., Krebs, W., et al. (2012). Lack of PPARγ in myeloid cells confers resistance to Listeria monocytogenes infection. PLoS ONE *7*, e37349, http://dx.doi.org/10.1371/journal.pone.0037349.

Al Dahouk, S., Jubier-Maurin, V., Scholz, H.C., Tomaso, H., Karges, W., Neubauer, H., and Köhler, S. (2008). Quantitative analysis of the intramacrophagic *Brucella suis* proteome reveals metabolic adaptation to late stage of cellular infection. Proteomics *8*, 3862–3870.

Alton, G.G., Jones, L.M., and Pietz, D.E. (1975). Laboratory Techniques in Brucellosis, Second Edition (Geneva: World Health Organization).

Barbier, T., Nicolas, C., and Letesson, J.J. (2011). *Brucella* adaptation and survival at the crossroad of metabolism and virulence. FEBS Lett. *585*, 2929–2934.

Bensinger, S.J., and Tontonoz, P. (2008). Integration of metabolism and inflammation by lipid-activated nuclear receptors. Nature *454*, 470–477.

Chawla, A. (2010). Control of macrophage activation and function by PPARs. Circ. Res. *106*, 1559–1569.

Copin, R., Vitry, M.-A., Hanot Mambres, D., Machelart, A., De Trez, C., Vanderwinden, J.-M., Magez, S., Akira, S., Ryffel, B., Carlier, Y., et al. (2012). In situ microscopy analysis reveals local innate immune response developed around *Brucella* infected cells in resistant and susceptible mice. PLoS Pathog. *8*, e1002575, http://dx.doi.org/10.1371/journal.ppat.1002575.

Eisele, N.A., Ruby, T., Jacobson, A., Manzanillo, P.S., Cox, J.S., Lam, L., Mukundan, L., Chawla, A., and Monack, D. (2013). Persistent *Salmonella* infection is controlled by PPARδ, a host regulator of fatty acid metabolism. Cell Host Microbe *14*, this issue, 171–182.

Essenberg, R.C., Candler, C., and Nida, S.K. (1997). Brucella abortus strain 2308 putative glucose and galactose transporter gene: cloning and characterization. Microbiology *143*, 1549–1555.

Fernandes, D.M., Jiang, X., Jung, J.H., and Baldwin, C.L. (1996). Comparison of T cell cytokines in resistant and susceptible mice infected with virulent *Brucella abortus* strain 2308. FEMS Immunol. Med. Microbiol. *16*, 193–203.

Fretin, D., Fauconnier, A., Köhler, S., Halling, S., Léonard, S., Nijskens, C., Ferooz, J., Lestrate, P., Delrue, R.M., Danese, I., et al. (2005). The sheathed flagellum of *Brucella melitensis* is involved in persistence in a murine model of infection. Cell. Microbiol. *7*, 687–698.

Gordon, S., and Martinez, F.O. (2010). Alternative activation of macrophages: mechanism and functions. Immunity *32*, 593–604.

Gorvel, J.P., and Moreno, E. (2002). *Brucella* intracellular life: from invasion to intracellular replication. Vet. Microbiol. *90*, 281–297.

Hong, P.C., Tsolis, R.M., and Ficht, T.A. (2000). Identification of genes required for chronic persistence of *Brucella abortus* in mice. Infect. Immun. *68*, 4102–4107.

Kohler, S., Foulongne, V., Ouahrani-Bettache, S., Bourg, G., Teyssier, J., Ramuz, M., and Liautard, J.P. (2002). The analysis of the intramacrophagic virulome of *Brucella suis* deciphers the environment encountered by the

pathogen inside the macrophage host cell. Proc. Natl. Acad. Sci. USA *99*, 15711–15716.

Lawrence, T., and Natoli, G. (2011). Transcriptional regulation of macrophage polarization: enabling diversity with identity. Nat. Rev. Immunol. *11*, 750–761.

Mahajan, S., Dkhar, H.K., Chandra, V., Dave, S., Nanduri, R., Janmeja, A.K., Agrewala, J.N., and Gupta, P. (2012). Mycobacterium tuberculosis modulates macrophage lipid-sensing nuclear receptors PPARγ and TR4 for survival. J. Immunol. *188*, 5593–5603.

Martirosyan, A., Moreno, E., and Gorvel, J.-P. (2011). An evolutionary strategy for a stealthy intracellular *Brucella* pathogen. Immunol. Rev. *240*, 211–234.

McCullough, N.B., and Beal, G.A. (1951). Growth and manometric studies on carbohydrate utilization of *Brucella*. J. Infect. Dis. *89*, 266–271.

McKinney, J.D., Höner zu Bentrup, K., Muñoz-Elías, E.J., Miczak, A., Chen, B., Chan, W.-T., Swenson, D., Sacchettini, J.C., Jacobs, W.R., Jr., and Russell, D.G. (2000). Persistence of *Mycobacterium tuberculosis* in macrophages and mice requires the glyoxylate shunt enzyme isocitrate lyase. Nature *406*, 735–738.

Odegaard, J.I., Ricardo-Gonzalez, R.R., Goforth, M.H., Morel, C.R., Subramanian, V., Mukundan, L., Red Eagle, A., Vats, D., Brombacher, F., Ferrante, A.W., and Chawla, A. (2007). Macrophage-specific PPARgamma controls alternative activation and improves insulin resistance. Nature *447*, 1116–1120.

O'Neill, L.A.J., and Hardie, D.G. (2013). Metabolism of inflammation limited by AMPK and pseudo-starvation. Nature *493*, 346–355.

Rafiei, A., Ardestani, S.K., Kariminia, A., Keyhani, A., Mohraz, M., and Amirkhani, A. (2006). Dominant Th1 cytokine production in early onset of human brucellosis followed by switching towards Th2 along prolongation of disease. J. Infect. *53*, 315–324.

Reyes, J.L., and Terrazas, L.I. (2007). The divergent roles of alternatively activated macrophages in helminthic infections. Parasite Immunol. *29*, 609–619.

Rolán, H.G., and Tsolis, R.M. (2007). Mice lacking components of adaptive immunity show increased *Brucella abortus virB* mutant colonization. Infect. Immun. *75*, 2965–2973.

Rolán, H.G., and Tsolis, R.M. (2008). Inactivation of the type IV secretion system reduces the Th1 polarization of the immune response to *Brucella abortus* infection. Infect. Immun. *76*, 3207–3213.

Rolán, H.G., Xavier, M.N., Santos, R.L., and Tsolis, R.M. (2009). Natural antibody contributes to host defense against an attenuated *Brucella abortus virB* mutant. Infect. Immun. *77*, 3004–3013.

Shi, C., and Pamer, E.G. (2011). Monocyte recruitment during infection and inflammation. Nat. Rev. Immunol. *11*, 762–774.

Shirey, K.A., Cole, L.E., Keegan, A.D., and Vogel, S.N. (2008). *Francisella tularensis* live vaccine strain induces macrophage alternative activation as a survival mechanism. J. Immunol. *181*, 4159–4167.

Starr, T., Ng, T.W., Wehrly, T.D., Knodler, L.A., and Celli, J. (2008). *Brucella* intracellular replication requires trafficking through the late endosomal/lysosomal compartment. Traffic *9*, 678–694.

Szanto, A., Balint, B.L., Nagy, Z.S., Barta, E., Dezso, B., Pap, A., Szeles, L., Poliska, S., Oros, M., Evans, R.M., et al. (2010). STAT6 transcription factor is a facilitator of the nuclear receptor PPARγ-regulated gene expression in macrophages and dendritic cells. Immunity *33*, 699–712.

Van Dyken, S.J., and Locksley, R.M. (2013). Interleukin-4- and Interleukin-13-mediated alternatively activated macrophages: roles in homeostasis and disease. Annu. Rev. Immunol. *31*, 31.

Vats, D., Mukundan, L., Odegaard, J.I., Zhang, L., Smith, K.L., Morel, C.R., Wagner, R.A., Greaves, D.R., Murray, P.J., and Chawla, A. (2006). Oxidative metabolism and PGC-1beta attenuate macrophage-mediated inflammation. Cell Metab. *4*, 13–24.

Wayne, L.G., and Lin, K.Y. (1982). Glyoxylate metabolism and adaptation of *Mycobacterium tuberculosis* to survival under anaerobic conditions. Infect. Immun. *37*, 1042–1049.

Yki-Järvinen, H. (2004). Thiazolidinediones. N. Engl. J. Med. *351*, 1106–1118.